Physica Scripta. Vol. T110, 299–301, 2004

Fine Structure in Cold Collisions of Spin-Polarized H(2s) Atoms

S. Jonsell[1,*], R. C. Forrey[2], A. Saenz[3], P. Froelich[4], and A. Dalgarno[5]

[1] Department of Physics, Umeå University, SE-90187 Umeå, Sweden
[2] Berks-Lehigh Valley College, Pennsylvania State University, Reading, Pennsylvania 19610-6009, USA
[3] Humboldt-Universität zu Berlin, Institut für Physik, AG Moderne Optik, Hausvogteiplatz 5–7, D-10117 Berlin, Germany
[4] Department of Quantum Chemistry, Uppsala University, Box 518, SE-75120 Uppsala, Sweden
[5] Institute for Theoretical Atomic and Molecular Physics, Harvard-Smithsonian Center for Astrophysics, 60 Garden Street, Cambridge, Massachusetts 02138, USA

Received July 3, 2003; accepted November 6, 2003

PACS ref: 31.50.-s, 03.75.Hh

Abstract

We have calculated cross sections and rate coefficients for elastic scattering, ionization, and double excitation transfer in collision of two hydrogen atoms in the 2s state. We find that for collision energies between 5×10^{-10} a.u. and 10^{-6} a.u. elastic scattering has the largest cross section. For temperatures below 0.02 K ionization is the dominant loss process, while for higher temperatures double excitation transfer dominates. Our results for the total loss rate are found to be within a factor 2 or 3 of the error bars of recent measurements.

In 1998 Bose–Einstein condensation of atomic hydrogen was achieved [1]. In this experiment two-photon spectroscopy of the 1s–2s line was used to probe the temperature and density of the condensate [2,3]. After recent improvements to the apparatus at MIT more than 10^7 metastable 2s atoms were generated at densities greater than $10^{10}\,\mathrm{cm}^{-3}$ and temperatures between 300 mK and 20 μK [4]. The natural life time of the 2s state is 0.122 s. At these densities the life time is, however, significantly reduced by collisional processes, known as collisional quenching. Understanding of these quenching processes is an important step towards using cold metastable hydrogen e.g. for precise measurements of fundamental constants and atom optics.

Our earlier calculations of scattering of H(2s) atoms at thermal energies [5] have recently been extended to the ultracold domain [6]. Collisional quenching occurs from associative ionization

$$\mathrm{H(2s)} + \mathrm{H(2s)} \rightarrow \mathrm{H_2^+} + \mathrm{e^-}, \tag{1}$$

Penning ionization

$$\mathrm{H(2s)} + \mathrm{H(2s)} \rightarrow \mathrm{H(1s)} + \mathrm{H^+} + \mathrm{e^-}, \tag{2}$$

and double excitation transfer

$$\mathrm{H(2s)} + \mathrm{H(2s)} \rightarrow \mathrm{H(2p)} + \mathrm{H(2p)}. \tag{3}$$

In our calculation the two ionization processes are not resolved.

The calculation of the molecular Σ states asymptotically correlating to $\mathrm{H}(n=2) + \mathrm{H}(n=2)$ was reported in Ref. [7]. Briefly, an explicitly correlated basis in prolate-spheroidal coordinates was used. Because of the ionization process these potentials are complex. The imaginary part of the potentials was calculated using a complex-scaling approach for diatomic molecules [8].

* e-mail: jonsell@tp.umu.se

We consider scattering of the H(2s) atoms with parallel spins of the electrons (couplings to nuclear angular momenta are neglected). Asymptotically this corresponds to the atomic product state

$$\phi_1 = |2,0,0\rangle|2,0,0\rangle\chi_{11}, \tag{4}$$

where $|n,l,m\rangle$ denotes the state of a hydrogen atom with principal quantum number n, angular momentum l, and projection of the angular momentum m, and χ_{SM_S} is the spin function for two electrons with total spin S and projection M_S. This state has the symmetry $^3\Sigma_u^+$ in the LS coupling scheme. Since the 2s and 2p states are almost degenerate, the molecular interaction strongly couples the state ϕ_1 to states of the same molecular symmetry asymptotically including 2p atoms. In total there are four such $^3\Sigma_u^+$ states, but it turns out that states asymptotically including one 2s and one 2p atom do not couple to the other states at large internuclear separations [9]. Hence, the single excitation transfer process, $\mathrm{H(2s)} + \mathrm{H(2s)} \rightarrow \mathrm{H(2s)} + \mathrm{H(2p)}$ is expected to have a very small cross section. We are therefore left with three relevant $^3\Sigma_u^+$ states, the complex potentials of which are shown in Fig. 1. The additional atomic product states are

$$\phi_2 = |2,1,0\rangle|2,1,0\rangle\chi_{11}, \tag{5}$$

$$\phi_3 = \frac{1}{\sqrt{2}}(|2,1,1\rangle|2,1,-1\rangle + |2,1,-1\rangle|2,1,1\rangle)\chi_{11}. \tag{6}$$

At low energies it is necessary to take the splitting between the $n=2$ atomic states into account. The splitting $\varepsilon = 1.61 \times 10^{-7}$ a.u. between the $2p_{1/2}$ and the $2s_{1/2}$ states is due to the Lamb shift, while the larger splitting $\delta = 1.67 \times 10^{-6}$ a.u. between the $2p_{1/2}$ and the $2p_{3/2}$ states is due to fine structure. Hence, to describe the atomic product states including these splittings we need to use the *jj* representation. The relevant asymptotic atomic product states are shown in Fig. 2. For $\mathrm{H(2s)} + \mathrm{H(2s)}$ scattering at energies less than $\delta - 2\varepsilon$ the inelastic $\mathrm{H}(2p_{1/2}) + \mathrm{H}(2p_{1/2})$ channel is open, while channels involving $\mathrm{H}(2p_{3/2})$ atoms are closed.

In the *jj* representation the molecular states are classified according to gerade/ungerade symmetry and projection of the total angular momentum of the electrons $\Omega = \Lambda + \Sigma$, where Λ is the projection of the orbital angular momentum, and Σ is the projection of the spin. For two spin-polarized H(2s) atoms the symmetry is $\Omega = 1$, ungerade. At short internuclear separations the fine structure and

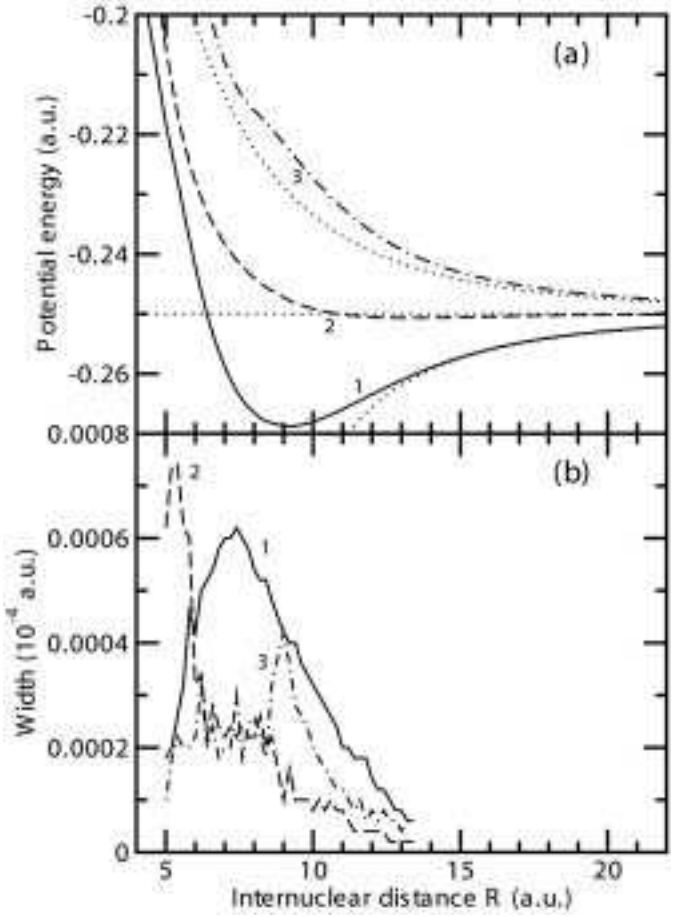

Fig. 1. Potentials for the three relevant $^3\Sigma_u^+$ potentials, (a) real energy, (b) width. The dotted curves in (a) show the asymptotic energy calculated using perturbation theory.

Lamb shift are negligible compared to the separation between the different potentials. Hence, the potentials in the *LS* representation are good approximations for separations of the order of 20 a.u. or less. However, due to the spin-orbit coupling it is not sufficient to consider Σ states only, but also Π and Δ states corresponding to the projection of total electronic angular momentum $\Omega = 1$. We find that three more molecular states with symmetries $^3\Pi_u$, $^1\Pi_u$, and $^3\Delta_u$ couple to the initial channel (4). The potentials for these states were calculated using a Feshbach projection technique [10], and are displayed in Fig. 3.

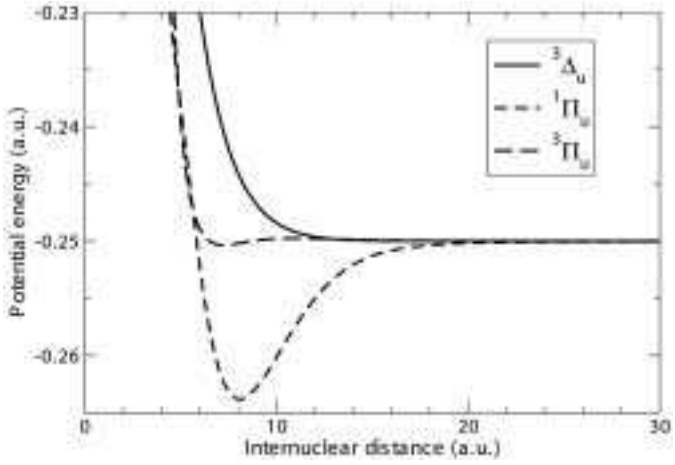

Fig. 3. Π and Δ potentials that couple to the initial state of two spin-polarized H(2s) atoms through spin-orbit coupling.

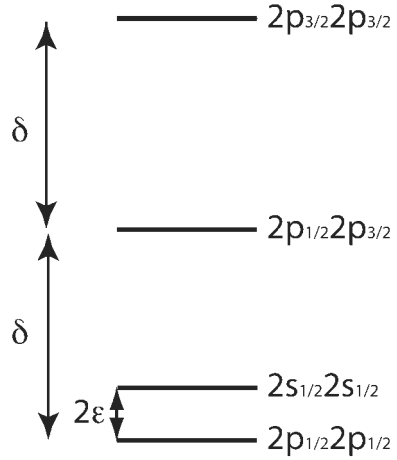

Fig. 2. Atomic product states relevant for scattering of spin-polarized H(2s) atoms.

Asymptotically these potentials correspond to the following atomic product states,

$$\phi_4 = \frac{1}{\sqrt{2}}(|2,1,0\rangle|2,1,1\rangle + |2,1,1\rangle|2,1,0\rangle)\chi_{10}, \tag{7}$$

$$\phi_5 = \frac{1}{\sqrt{2}}(|2,1,0\rangle|2,1,1\rangle - |2,1,1\rangle|2,1,0\rangle)\chi_{00}, \tag{8}$$

$$\phi_6 = \frac{1}{\sqrt{2}}|2,1,1\rangle|2,1,1\rangle\chi_{1\text{-}1}. \tag{9}$$

We are left with six coupled potentials. Although some coupling exist at all internuclear distances R, for $R \lesssim 20$ a.u. the energy differences between the potentials are much larger than the typical couplings, and hence the transition amplitude between potentials will be small. In this region we therefore use the adiabatic potentials calculated in the *LS* representation, ignoring couplings between the potentials. For large internuclear distances the situation is quite different, the couplings between potentials are of the same order of magnitude as the fine structure splitting, and a large number of avoided crossings occur between the adiabatic potentials. Here the leading contributions to both potentials and couplings can be calculated using first-order perturbation theory. Additionally the fine-structure split-

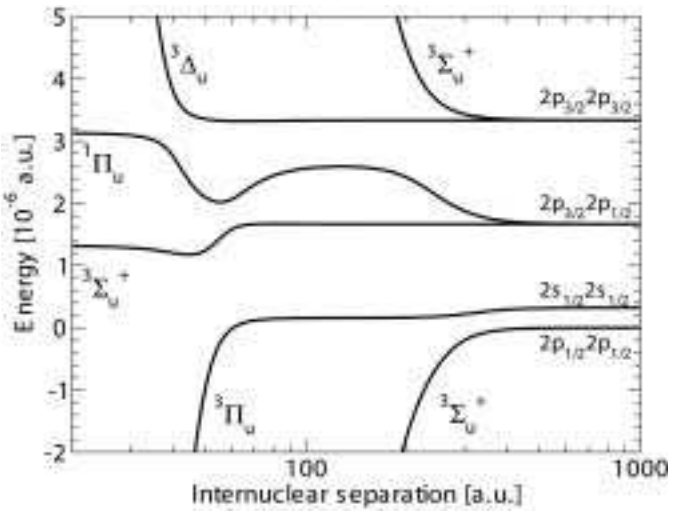

Fig. 4. Long-range adiabatic potentials including splitting between atomic states due to fine structure and Lamb shift.

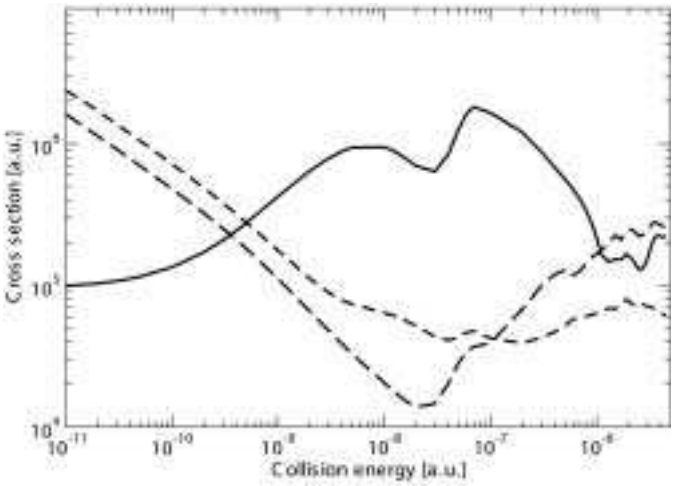

Fig. 5. Cross sections for scattering of spin-polarized H(2s) atoms, elastic scattering (solid curve), ionization (short dashed curve), and double excitation transfer (long dashed curve).

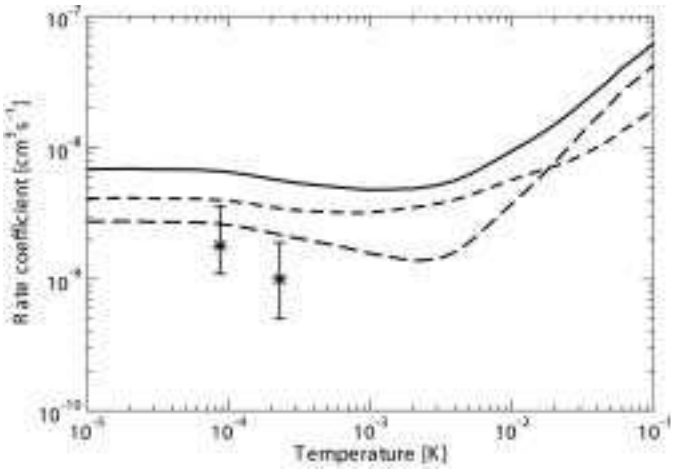

Fig. 6. Loss rate coefficient for ionization (short dashed curve), double excitation transfer (long dashed curve), and total loss (solid curve). The stars show experimental results from Ref. [4]

ting δ and Lamb shift ε must be included. In the representation defined by the atomic product states ϕ_i [Eqs. (4–9)] the asymptotic interaction is given by the matrix

$$V = \begin{pmatrix} 2\varepsilon & -\frac{18}{R^3} & -\frac{9\sqrt{2}}{R^3} & 0 & 0 & 0 \\ -\frac{18}{R^3} & \frac{4\delta}{3}+\frac{864}{R^5} & \frac{432\sqrt{2}}{R^5} & \frac{\sqrt{2}\delta}{3} & \frac{\sqrt{2}\delta}{3} & 0 \\ -\frac{9\sqrt{2}}{R^3} & \frac{432\sqrt{2}}{R^5} & \frac{4\delta}{3}+\frac{432}{R^5} & \frac{\delta}{3} & -\frac{\delta}{3} & 0 \\ 0 & \frac{\sqrt{2}\delta}{3} & \frac{\delta}{3} & \frac{4\delta}{3}-\frac{864}{R^5} & -\frac{\delta}{3} & \frac{\sqrt{2}\delta}{3} \\ 0 & \frac{\sqrt{2}\delta}{3} & -\frac{\delta}{3} & -\frac{\delta}{3} & \frac{4\delta}{3} & \frac{\sqrt{2}\delta}{3} \\ 0 & 0 & 0 & \frac{\sqrt{2}\delta}{3} & \frac{\sqrt{2}\delta}{3} & \frac{2\delta}{3}+\frac{216}{R^5} \end{pmatrix}. \tag{10}$$

Note that fine structure and Lamb shift also gives non-diagonal interactions in the *LS* representation, although it is diagonal in the *jj* representation. In fact if one sets $\delta = 0$ then the couplings to Π and Δ states vanish, as one would expect when spin-orbit couplings are neglected. Figure 4 shows the six adiabatic potentials that result from diagonalization of V.

The scattering calculation uses the matrix V transformed to the *jj* representation, and matched to the complex interaction potentials in the *LS* representation at short internuclear distances. This results in six coupled Schrödinger equations which are solved using multichannel Numerov propagation. The resulting low-energy cross sections for elastic scattering, ionization (1,2), and double excitation transfer (3) are displayed in Fig. 5. For energies $5 \times 10^{-10} < E < 10^{-6}$ a.u. elastic scattering dominates. As required by threshold laws the elastic cross section is constant at low energies, while the inelastic cross sections diverge as $E^{-1/2}$. In the zero-energy limit the scattering properties can be summarized by the scattering length $a_{22} = 33 - 22i$ Å.

In Fig. 6 we show the temperature averaged loss rates. The loss rate is twice the scattering rate because two atoms are lost in each scattering event. Ionization is the dominating inelastic process for temperatures < 0.02 K. The total loss rate is compared to the experimental values from Ref. [4]. Our theoretical values are within a factor of 2 or 3 of the experimental error bars. The discrepancy could be due to effects not included in the theoretical calculations, such as the hyperfine interaction, nonadiabatic couplings, and magnetic field dependencies of the potentials. These effects will be the subject of future work.

Acknowledgments

The research has been supported by the National Science Foundation through grants to the Center for Ultracold Atoms, the Institute for Theoretical Atomic and Molecular Physics, and Grant No. PHY-0070920 to R.C.F. S.J. and P.F. acknowledge support by the Swedish Research Council, A.S. acknowledges support by the Deutsche Forschungsgemeinschaft (DFG) in the framework of SPP 1116, and A.D. acknowledges support by the Chemical Sciences, Geoscience and Biosciences Division of the Office of Basic Engineering Sciences, U.S. Department of Energy.

References

1. Fried, D. G. *et al.*, Phys. Rev. Lett. **81**, 3811 (1998).
2. Cesar, C. L. *et al.*, Phys. Rev. Lett. **77**, 255 (1996).
3. Killian, T. C. *et al.*, Phys. Rev. Lett. **81**, 3807 (1998).
4. Landhuis, D. *et al.*, Phys. Rev. A **67**, 022718 (2003).
5. Forrey, R. C. *et al.*, Phys. Rev. Lett. **85**, 4245 (2000).
6. Forrey, R. C. *et al.* Phys. Rev. A **67**, 040701 (2003).
7. Jonsell, S. *et al.*, Phys. Rev. A **65**, 042501 (2002).
8. Froelich, P., Jeziorski, B., Kolos, W., Saenz, A. and Monkhorst, H. J., Phys. Rev. Lett. **71**, 2871 (1993).
9. Nikitin, S. I., Ostrovskii, V. N. and Prudov N. V., Sov. Phys. JETP **64**, 745 (1986).
10. Saenz, A. *et al.*, in preparation.